THE ASTROPHYSICAL JOURNAL, 507:L135–L139, 1998 November 10

FOSSIL IMPRINTS OF THE FIRST-GENERATION SUPERNOVA EJECTA IN EXTREMELY METAL-DEFICIENT STARS

TOSHIKAZU SHIGEYAMA
Department of Astronomy and Research Center for the Early Universe, Graduate School of Science, University of Tokyo, Bunkyo-ku, Tokyo 113-0033, Japan; shigeyama@astron.s.u-tokyo.ac.jp
AND
TAKUJI TSUJIMOTO
National Astronomical Observatory, Mitaka-shi, Tokyo 181-8588, Japan; tsuji@misty.mtk.nao.ac.jp
Received 1998 July 8; accepted 1998 September 14; published 1998 September 29

ABSTRACT

Using the results of nucleosynthesis calculations for theoretical core-collapse supernova models with various progenitor masses, it is shown that the abundance patterns of C, Mg, Si, Ca, and H that are seen in extremely metal-deficient stars with [Fe/H] $\lesssim -2.5$ follow those seen in the individual first-generation supernova remnants (SNRs). This suggests that most of the stars with [Fe/H] $\lesssim -2.5$ were made from individual supernova (SN) events. To obtain the ratio of heavy elements to hydrogen, a formula is derived to estimate the mass of hydrogen swept up by an SNR when it occurs in the interstellar matter with the primordial abundances. We use [Mg/H] to indicate the metallicities instead of [Fe/H]. The metallicities [Mg/H] predicted from these SNRs range from ~ -4 to ~ -1.5, and the mass of Mg in an SN is well correlated with its progenitor mass. Thus, the observed [Mg/H] in an extremely metal-deficient star has a correspondence to the progenitor mass. A larger [Mg/H] corresponds to a larger progenitor mass. Therefore, the so-called "age-metallicity relation" does not hold for stars with [Fe/H] $\lesssim -2.5$. In contrast, the [Mg/Fe] ratios in the theoretical SNRs have a different trend from those in extremely metal-deficient stars. It is also shown that from the observed trend of [Mg/Fe], one can predict the Fe yield of each SN given the correspondence of [Mg/H] to the progenitor mass. The Fe yields thus obtained are consistent with those derived from SN light-curve analyses. This indicates that there is still a problem in modeling a core-collapse supernova at the beginning of its explosion or mass cut. The abundance determination of O in extremely metal-deficient stars, which has not been done from observational analyses, is strongly desired in order to test the hypothesis that the elements in an extremely metal-deficient star come from a single SN event and to obtain reliable yields for SNe.

Subject headings: nuclear reactions, nucleosynthesis, abundances — stars: abundances — stars: Population II — supernovae: general — supernova remnants

1. INTRODUCTION

Recent observations and analyses imply that the abundance pattern of an extremely metal-deficient star with [Fe/H] $\lesssim -2.5$ may retain information of a preceding single supernova (SN) event or, at most, a few SNe (McWilliam et al. 1995; Ryan, Norris, & Beers 1996). A theoretical attempt from this point of view has already been made by Audouze & Silk (1995) to explain the observed abundance patterns. They argued that a combination of yields from two SNe with different progenitor masses at the main sequence ($M_{\rm ms}$) is consistent with the abundance patterns of stars with the lowest metallicity ([Fe/H] ~ -4).

Assuming that the formation of extremely metal-deficient stars is triggered by a single supernova remnant (SNR) and that the formed stars retain the abundance pattern of this SN, one could predict the abundance patterns (including hydrogen) of these stars from the theoretical SN models available at present (see, e.g., Woosley & Weaver 1995; Tsujimoto et al. 1995; Nomoto et al. 1997). In this Letter, we will compare the abundance pattern obtained in this way with observations, in order to test whether the chemical enrichment by individual SNRs could explain the observed abundances on the surfaces of extremely metal-deficient stars. We will use the models in Woosley & Weaver (1995, hereafter WW95) and those in Tsujimoto et al. (1995, hereafter T95) and Nomoto et al. (1997).

The metallicity of a star has usually been indicated by [Fe/H]. On the other hand, the yields of Fe from SN models to date have not converged (WW95; T95) because of uncertainties in the explosion mechanism and fallback dynamics or because of the mass cut between the forming neutron star (or black hole) and the ejected envelope (see, e.g., Thielemann, Hashimoto, & Nomoto 1990). Thus, the yields of lighter α-elements are more reliably calculated. We will use [Mg/H] instead of [Fe/H] to specify the metallicity because (1) Mg is less affected by the mass cut in SN models than Fe is, (2) Mg is not synthesized or broken by the SN shock, (3) the mass of ejected Mg increases with increasing progenitor mass, and (4) the abundance of Mg is observationally derived for many stars with [Fe/H] $\lesssim -2.5$. There is a disadvantage in this element; i.e., two SN models (WW95 and T95) give somewhat different masses of Mg as a function of the progenitor mass (Fig. 1, *squares*). The best element to be used in this respect would be O (Fig. 1, *pentagons*) if O abundances were available for many stars with [Fe/H] $\lesssim -2.5$.

There is a clear trend in the observed [C/Mg]-[Mg/H] plot (Fig. 2, *crosses*) for [Mg/H] < -2 that cannot be reconciled with the conventional one-zone models of the Galactic chemical evolution that assume a complete mixing of elements inside the Galaxy. The difference of the observed [C/Mg] in the range of $-3.5 \lesssim$ [Mg/H] $\lesssim -2$ gives a mean gradient of Δ[C/Mg]/Δ[Mg/H] ~ -0.7. On the other hand, the one-zone Galactic chemical evolution model (T95) would predict the evolutionary change in [C/Mg] starting with the value of ~ -1.2 given by the most massive star ($M_{\rm ms} \sim 50\ M_\odot$) and converging

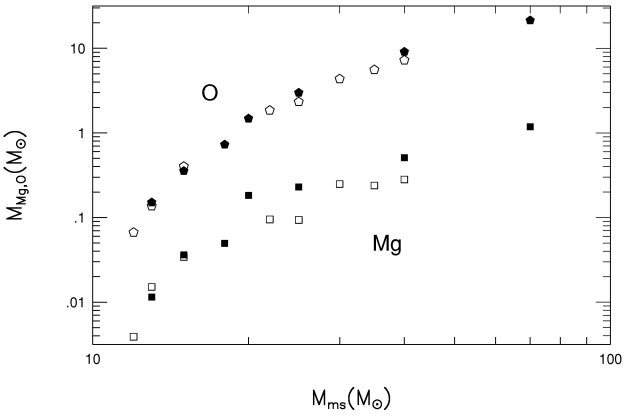

FIG. 1.—The masses of Mg (*squares*) and O (*pentagons*) ejected from SN models are plotted as a function of the progenitor mass (WW95 [*open*]; T95 [*filled*]).

to the average value of ~ -0.9 integrated for stars in the mass range of $10 < M_{ms}/M_\odot < 50$ over the Salpeter initial mass function (IMF) with a slope of $x = -1.35$. It results in the corresponding gradient of Δ[C/Mg]/Δ[Mg/H] ~ 0.2 that has the opposite sign and a smaller absolute value than in observations. This argument also holds for WW95. If we introduce a metallicity-dependent IMF, the observed gradient requires a drastic change of the slope of the IMF from $x \sim -10$ at [Fe/H] ~ -4 to $x \sim 0.5$ at [Fe/H] ~ -2.5. The index of $x \sim -10$ is almost equivalent to assuming that most of the stars with [Fe/H] ~ -4 are formed from SNRs with $M_{ms} = 10\ M_\odot$. It will be shown in the following section that this is indeed the case if we assume that most of the stars with [Fe/H] $\lesssim -2.5$ are formed from individual SN events.

Here we will also predict the Fe yields as a function of M_{ms} using the observed [Mg/Fe]-[Mg/H] trend combined with the [Mg/H]-M_{ms} relation in theoretical SN models. Then these Fe yields are compared with those derived from SN light-curve analyses. To calculate the mass of hydrogen swept up by an SNR, which is important for obtaining [Mg/H], the analytical expression for this mass in Cioffi, Mckee, & Bertschinger (1988) is modified to be applicable to SNRs that occur in metal-free interstellar matter (ISM).

2. LATE-STAGE EVOLUTION OF THE FIRST-GENERATION SNR

In a spherically symmetric SNR (see, e.g., Cioffi et al. 1988), after the radiative cooling timescale becomes shorter than the dynamical timescale at the shock front, the shock front propagates considerably slower than before and makes a dense shell immediately behind it. Most of the mass inside the shock front resides in this shell. The ejecta that contain heavy elements occupy only a small central portion of the SNR, even during this pressure-driven snowplow (PDS) phase. In a realistic SNR, the situation is different. First, the contact surface between the ejecta and the ISM is subject to the Rayleigh-Taylor instability during the preceding Sedov-Taylor phase (Taylor 1950; Sedov 1959). A large part of the ejecta penetrates into the ISM. Thus, it is expected that the ejecta already approach the dense shell at the beginning of the PDS phase and merge with it during this phase. Second, an isothermal shock front is considered to be dynamically unstable (Vishniac 1983). Thus, the dense shell behind the shock front is fragmented into a number of cloud cores that retain the abundance pattern of the SN. These cloud

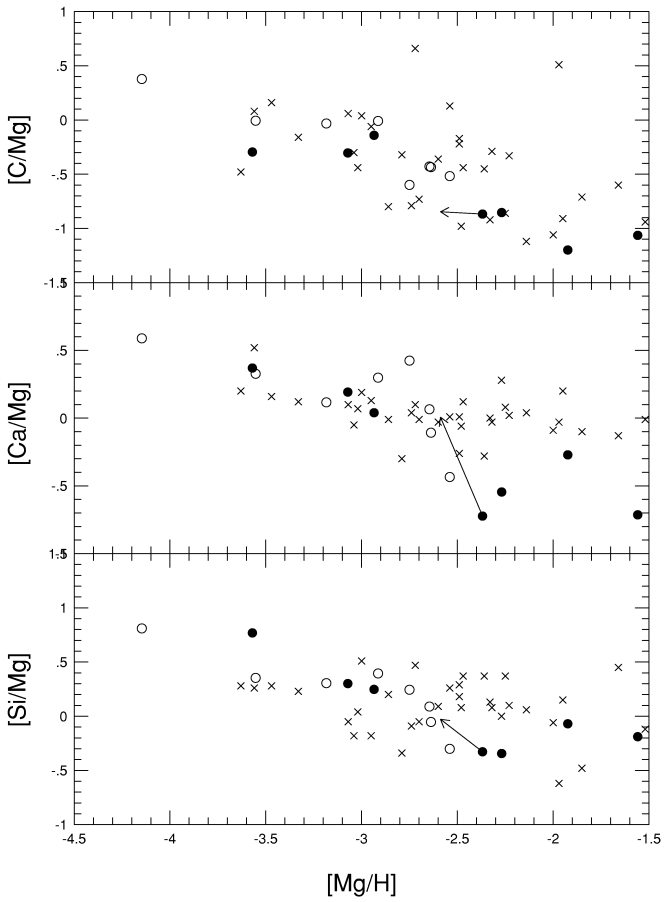

FIG. 2.—*Top panel*: the crosses are the observed [C/Mg] for stars plotted against [Mg/H] (McWilliam et al. 1995). The open and filled circles show the same quantities in the first-generation SNRs calculated from theoretical SN models (WW95 [*open circles*]; T95 [*filled circles*]). The arrow indicates the change in the abundance pattern of the model so as to reproduce the SN 1987A observations (Thielemann et al. 1990 and references therein). *Middle panel*: same as the top panel, but for [Ca/Mg]. *Bottom panel*: same as the top panel, but for [Si/Mg]. See text for arrows.

cores embedded in a high ambient pressure become seeds of stars of the next generation (Nakano 1998). Some of the stars thus formed are currently observed as extremely metal-deficient stars. Accordingly, the average abundance pattern inside the SNR is assumed to represent the abundance pattern in all these stars.

Cioffi et al. (1988) obtained the time t_{merge} when an SNR loses its identity. This time is a function of the ratio of the shock velocity to the sound speed c_s (or the velocity dispersion) of the ISM at the beginning of the PDS phase ($t = t_{PDS}$) and t_{PDS} itself. For an SNR in a homogeneous ISM with the density of n_1, t_{PDS} is determined by

$$\frac{1}{n_1}\frac{\partial e}{\partial t} = -\alpha\Lambda(T), \tag{1}$$

where e and $\Lambda(T)$ are the internal energy and the cooling function at the temperature T, respectively. All the variables are evaluated at the shock front using Sedov-Taylor solutions for the point explosion with the energy E_0 and the number density n_1. The constant α should be equal to 1.85 in order to reproduce t_{PDS} for the numerical simulation in Cioffi et al. (1988) when

$\Lambda(T)$ for the solar abundances is used. Then $\Lambda_{\rm primordial}(T)$ is constructed for the gas composed of only hydrogen and helium, with their mass ratio $X_{\rm H}$:$X_{\rm He}$ = 0.75:0.25 under the collisional ionization equilibrium. For $n_1 \gtrsim 10^{-2}$ cm^{-3}, equation (1) gives $T > 10^5$ K. Thus, the ionization of hydrogen does not affect the dynamics.

The mass of hydrogen $M_{\rm sw}$ thus obtained with $\Lambda(T) = \Lambda_{\rm primordial}(T)$ in equation (1) is approximated by the formula

$$M_{\rm sw} = 5.1 \times 10^4\, M_\odot \left(\frac{E_0}{10^{51}\ {\rm ergs}}\right)^{0.97} \times\, n_1^{-0.062} \left(\frac{c_s}{10\ {\rm km\ s^{-1}}}\right)^{-9/7}. \quad (2)$$

The $M_{\rm sw}$ is insensitive to n_1. The sound speed c_s was assumed to be 10 km s^{-1} (or $T \sim 10^4$ K). This mass depends on E_0 and n_1 in a different way than that of Cioffi et al. (1988) because of the different cooling function used here. The cooling function with the primordial abundances is approximately proportional to T^{-2} instead of $T^{-1/2}$ in Cioffi et al. (1988).

3. ABUNDANCE PATTERNS IN EXTREMELY METAL-POOR STARS

Here we assume that all the stars with [Mg/H] < -2 are made from individual SNRs. Abundance patterns in individual SNRs will be calculated based on yields from theoretical SN models and will be compared with those on the surface of metal-deficient stars obtained by McWilliam et al. (1995). For SN models in a metal-free environment, we use the models Z12A, Z13A, Z15A, Z22A, Z30B, Z35C, and Z40C in WW95 to retain the monotonicity of the mass of Mg as a function of the progenitor mass (Fig. 1, *filled squares*). Another group of SN models is taken from T95, in which the initial metallicity is solar. The parameters of both models are listed in Table 1.

We divide elements into two categories. One category is composed of the elements not (or at least less) affected by the mass cut in SN models. The examples are C, Mg, Si, and Ca. The other is composed of those affected by the mass cut and includes Cr, Mn, Fe, Co, Ni, for example. This division is necessary because the mass cut in SN models to date is totally artificial and uncertain.

Elements not influenced by the mass cut.—The yields of elements not influenced by the mass cut are expected to be more reliably calculated in SN models than those influenced by the mass cut. Therefore, observed abundance ratios of [C/Mg], [Ca/Mg], and [Si/Mg] with respect to [Mg/H] (Fig. 2) can tell whether extremely metal-deficient stars were formed from individual SNe. These abundance ratios that were derived from SN models (*open circles*: WW95; *filled circles*: T95) are also plotted in the same figure, in which [Mg/H] is calculated from the ratio of the mass of Mg in an SNR to that of hydrogen swept up by the same SNR (see eq. [2]). The relations between [Mg/H] and $M_{\rm ms}$ are shown in Table 1 for both SN models. The values of [Mg/H] for $M_{\rm ms} \sim 10\ M_\odot$ (the lower mass limit of the core-collapse SN progenitor) from both models are not so far from the observed lowest value of [Mg/H] ~ -3.7, and the metallicity [Mg/H] increases with increasing progenitor mass $M_{\rm ms}$. From this, we infer that there are more stars at lower metallicities according to an IMF that decreases toward high masses if stars with lower masses, say 10 $M_\odot$, explode in the regions that have not been polluted by other SNRs before. This condition is represented as $n_\star V_{\rm SNR} \int_{10\,M_\odot}^{50\,M_\odot} \phi(m)dm < 1$ star. Here

TABLE 1

INPUT PARAMETERS IN SN MODELS AND CALCULATED [Mg/H] RATIOS IN CORRESPONDING SNRs

	WW95			T95		
NAME	$M_{\rm ms}$ ($M_\odot$)	E_0 ($\times 10^{51}$ ergs)	[Mg/H]	$M_{\rm ms}$ ($M_\odot$)	E_0 ($\times 10^{51}$ ergs)	[Mg/H]
Z12A	12	1.28	−4.1	13	1	−3.6
Z13A	13	1.29	−3.6	15	1	−3.1
Z15A	15	1.27	−3.2	18	1	−2.9
Z22A	22	1.26	−2.8	20	1	−2.4
Z25B	25	1.83	−2.9	25	1	−2.3
Z30B	30	2.06	−2.5	40	1	−1.9
Z35C	35	2.49	−2.6	70	1	−1.6
Z40C	40	3.01	−2.6	...	...	...

$n_\star$, ϕ, and $V_{\rm SNR}$ denote the number density of the first-generation stars, the IMF normalized to unity between the lower and upper mass limits, and the maximum volume occupied by a single SNR, respectively. This condition results in a star formation efficiency for the first-generation stars smaller than 2%, if the Salpeter IMF is used.

A trend seen in the observed [C/Mg] (the crosses in the top panel of Fig. 2) is well reproduced by both models. This means that stars with [Mg/H] ~ -3.5 were made from individual low-mass ($M_{\rm ms} \sim 10\ M_\odot$) SNe and that stars with [Mg/H] ~ -2 were from individual high-mass SNe ($M_{\rm ms} \sim 50\ M_\odot$). For [Si/Mg], both models are also consistent with the observations, although the observed [Si/Mg] has no clear trend. The [Ca/Mg] ratios derived from T95 with $M_{\rm ms} \geq 20\ M_\odot$ deviate from the observations and give lower values in the region [Mg/H] > -2.5. This indicates that the yields of Ca from T95 with $M_{\rm ms} \geq 20\ M_\odot$ are too small. These abundance patterns, together with the predicted [Mg/H] ratios in Table 1, suggest that stars with $-3.5 \lesssim$ [Mg/H] $\lesssim -2$ are made from individual SN events.

Elements influenced by the mass cut.—The top panel of Figure 3 shows that the [Mg/Fe] ratios derived from both models do not follow the observations. This reconfirms that none of the two models correctly describe the dynamics and/or nucleosynthesis near the surface of the Fe core in progenitor stars during the explosion. In both models, less massive stars have Fe yields that are too large. More massive stars in T95 have Fe yields that are too small, but the opposite is the case for WW95. The bottom panel of Figure 3 shows that the [Ca/Fe] ratios from both models are smaller than the observations. This can be ascribed to Fe yields that are too large, again from less massive stars of theoretical models. An apparent fit of the observational data to the model for [Mg/H] > -2.5 is a consequence of two errors in the yields of both Ca (see § 3) and Fe for more massive stars (see the next section).

Abundances of some heavy elements in the ejecta of the 20 $M_\odot$ supernova were deduced from the SN 1987A observations (Thielemann et al. 1990 and references therein). Since the mass of Mg that was ejected from SN 1987A was not estimated from the observations, we derive the mass of Mg by reducing the value of T95 to match the observed [Mg/Fe] ratio in extremely metal-deficient stars. The corresponding change of [Mg/Fe] is shown by the arrow in the top panel of Figure 3. If we use the mass of Mg derived in this way and the observed masses of C, Si, Fe, and Ca (the upper limit), the abundance ratios of the model with $M_{\rm ms} = 20\ M_\odot$ would move, following the arrows in Figure 2 and the arrows in the bottom panel of Figure 3. Thus, the abundance pattern of the best observed SN coincides

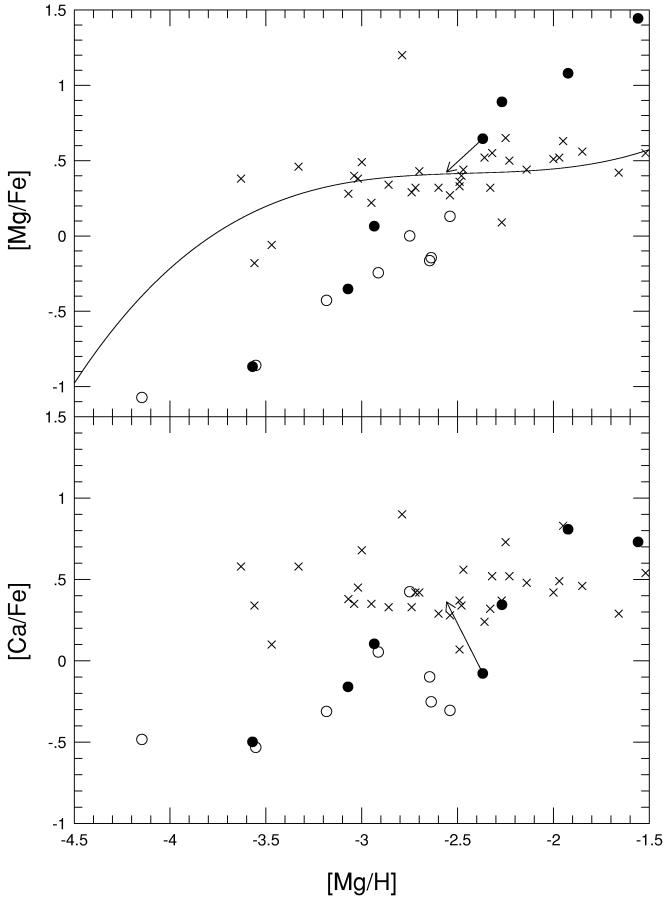

FIG. 3.—*Top panel*: the crosses are the observed [Mg/Fe] for stars plotted against [Mg/H] (McWilliam et al. 1995). The solid curve shows the χ^2 fit of the observed points, with the errors given in McWilliam et al. (1995), to a cubic polynomial formula. The open and filled circles show the same quantities in the first-generation SNRs calculated from theoretical SN models (WW95 [*open circles*]; T95 [*filled circles*]). *Bottom panel*: same as the top panel, but for [Ca/Fe]. See text for arrows.

with that in extremely metal-deficient stars with [Mg/H] ~ -2.6, and the mass of Mg in the 20 $M_\odot$ from T95 might be overestimated.

4. IRON YIELDS DEDUCED FROM EXTREMELY METAL-DEFICIENT STARS

We will reverse the argument in the preceding sections. Let us suppose that the trends in the observed abundance ratios, say [Mg/Fe], show yields of SNe as a function of [Mg/H]. The χ^2 fit of the observational data to a cubic polynomial formula gives the solid curve in the top panel of Figure 3. This curve and the [Mg/H] ratio of each model help us predict the mass of Fe ($M_{\rm Fe}$) from an SN as a function of $M_{\rm ms}$. The filled circles in Figure 4 show the predicted Fe masses using T95. These Fe masses are completely different from those given in the original models (*triangles*), but they hardly change the average Fe yield integrated over the Salpeter IMF. The open circles are those from WW95 and give a similar amount of Fe for each progenitor mass. The points with error bars, which are also

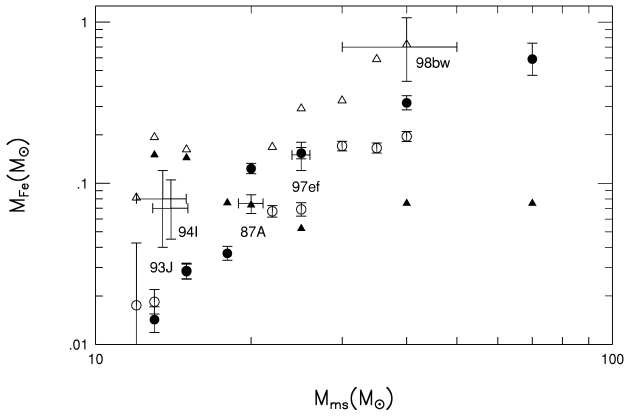

FIG. 4.—The masses of Fe in SN models (WW95 [*open*]; T5 [*filled*]) are shown by triangles. The circles show the masses of Fe in SN models with 1 σ error bars of the χ^2 fit in the top panel of Fig. 3. These masses are determined by the [Mg/Fe]-[Mg/H] relations, indicated with the solid curve in the top panel of Fig. 3, and the [Mg/H]-$M_{\rm ms}$ relations. The points with error bars are the masses of ^{56}Ni, which eventually decays to ^{56}Fe derived from the SN light-curve analyses (SN 1987A: Shigeyama & Nomoto 1990; SN 1993J: Shigeyama et al. 1994; SN 1994I: Iwamoto et al. 1994; SN 1997ef: Iwamoto et al. 1998a; SN 1998bw: Iwamoto et al. 1998b).

shown in the same figure, are the Fe masses obtained from SN light-curve analyses. Good fits of the Fe masses from the light-curve analyses to those inferred from the abundance patterns demonstrate that this procedure for obtaining the Fe yields works, if the Fe yields are not affected by the initial metallicities.

5. CONCLUSIONS

We have shown that the abundance patterns of C, Mg, Si, Ca, and H theoretically predicted in the first-generation SNRs are in good agreement with those observed in extremely metal-deficient stars with $-4 < [{\rm Fe/H}] < -2.5$. All these elements are thought to be less affected by the mass cut in SN modeling than heavier elements like Fe are. This agreement implies that each extremely metal-deficient star was formed from a single SN event. In contrast, both theoretical SN models predict different trends in the [Mg/Fe]-[Mg/H] plot from the observed one. Conversely, the mass of Fe that is ejected by each SN as a function of $M_{\rm ms}$ can be derived from the observed [Mg/Fe]-[Mg/H] trend combined with the [Mg/H]-$M_{\rm ms}$ relation in theoretical SN models. This $M_{\rm Fe}$ as a function of $M_{\rm ms}$ is consistent with that derived from SN light-curve analyses. Following the same procedure presented in this Letter for obtaining the Fe yields, we can derive the yields for other elements such as Ti, Cr, Mn, Co, and Ni and *r*-process elements (Tsujimoto & Shigeyama 1998), all of which are very uncertain in SN models. If O abundances are deduced in extremely metal-deficient stars, we will be able to obtain more reliable yields for SNe.

We are grateful to the anonymous referee for making useful comments. This work has been partially supported by the COE research (07CE2002) of the Ministry of Education, Science, Culture, and Sports in Japan.

REFERENCES

Audouze, J., & Silk, J. 1995, ApJ, 451, L49
Cioffi, D. F., Mckee, C. F., & Bertschinger, E. 1988, ApJ, 334, 252
Iwamoto, K., Nakamura, T., Nomoto, K., Mazzali, P. A., Garnavich, P., Kirshner, R., Jha, S., Balam, D. 1998a, ApJ, submitted
Iwamoto, K., Nomoto, K., Höflich, P., Yamaoka, H., Kumagai, S., & Shigeyama, T. 1994, ApJ, 437, L115
Iwamoto, K., et al. 1998b, Nature, in press
McWilliam, A., Preston, G. W., Sneden, C., & Searle, L. 1995, AJ, 109, 2757
Nakano, T. 1998, ApJ, 494, 587
Nomoto, K., Hashimoto, M., Tsujimoto, T., Thielemann, F.-K., Kishimoto, N., Kubo, Y., & Nakasato, N. 1997, Nucl. Phys. A, 616, 79c
Ryan, S. G., Norris, J. E., & Beers, T. C. 1996, ApJ, 471, 254
Sedov, L. I. 1959, Similarity and Dimensional Methods for Initial-Value Problems (New York: Wiley-Interscience)
Shigeyama, T., & Nomoto, K. 1990, ApJ, 360, 242
Shigeyama, T., Suzuki, T., Kumagai, S., Nomoto, K., Saio, H., & Yamaoka, H. 1994, ApJ, 420, 341
Taylor, G. I. 1950, Proc. R. Soc. London A, 201, 159
Thielemann, F.-K., Hashimoto, M., & Nomoto, K. 1990, ApJ, 349, 222
Tsujimoto, T., Nomoto, K., Yoshii, Y., Hashimoto, M., Yanagida, S., & Thielemann, F.-K. 1995, MNRAS, 277, 945 (T95)
Tsujimoto, T., & Shigeyama, T. 1998, ApJ, submitted
Vishniac, E. T. 1983, ApJ, 274, 152
Woosley, S. E., & Weaver, T. A. 1995, ApJS, 101, 181 (WW95)